OFFICE OF NAVAL RESEARCH

FINAL TECHNICAL REPORT

for

Grant: N00014-00-1-0165

PR Number: 01PR02906-00

VANADIUM OXIDE AEROGEL ELECTRODE MATERIALS

Professor Bruce Dunn

Department of Materials Science and Engineering
University of California, Los Angeles
Los Angeles, CA 90095-1595

March, 2001

Project Period: 1 December 1999 - 31 December 2000

20010323 060

REPORT DOCUMENTATION PAGE

Form Approved
OMB No. 0704-0188

Public reporting burden for this collection of information is estimated to average 1 hour per response, including the time for reviewing instructions, searching data sources, gathering and maintaining the data needed, and completing and reviewing the collection of information. Send comments regarding this burden estimate or any other aspect of this collection of information, including suggestions for reducing this burden to Washington Headquarters Service, Directorate for Information Operations and Reports, 1215 Jefferson Davis Highway, Suite 1204, Arlington, VA 22202-4302, and to the Office of Management and Budget, Paperwork Reduction Project (0704-0188) Washington, DC 20503.

PLEASE DO NOT RETURN YOUR FORM TO THE ABOVE ADDRESS.

1. REPORT DATE (DD-MM-YYYY)	2. REPORT DATE	3. DATES COVERED (From - To)
12/03/2001	Final Report	December 1999 – Dec 2001

4. TITLE AND SUBTITLE	5a. CONTRACT NUMBER
Vanadium Oxide Aerogel Electrode Materials	
	5b. GRANT NUMBER
	N00014-00-1-0165
	5c. PROGRAM ELEMENT NUMBER

6. AUTHOR(S)	5d. PROJECT NUMBER
Bruce Dunn	01PR02906-00
	5e. TASK NUMBER
	5f. WORK UNIT NUMBER

7. PERFORMING ORGANIZATION NAME(S) AND ADDRESS(ES)	8. PERFORMING ORGANIZATION REPORT NUMBER
Department of Materials Science and Engineering University of California, Los Angeles 405 Hilgard Avenue – Ste 1200, Wilshire Center Los Angeles, CA 90024-1406	

9. SPONSORING/MONITORING AGENCY NAME(S) AND ADDRESS(ES)	10. SPONSOR/MONITOR'S ACRONYM(S)
Office of Naval Research Ballston Center Tower One 800 North Quincy Street Alexandria, VA 22217-5660	
	11. SPONSORING/MONITORING AGENCY REPORT NUMBER

12. DISTRIBUTION AVAILABILITY STATEMENT

Approved for public release; distribution is unlimited

13. SUPPLEMENTARY NOTES

14. ABSTRACT

This research consists of two studies related to the incorporation of vanadium oxide aerogels in electrode structures for secondary lithium batteries. A common theme in this work is that the electrode structures retain their interconnected mesoporous morphology so that there is electrolyte access to the solid oxide phase. One series of experiments is directed at creating a nanocomposite electrode based on combining carbon nanotubes with vanadium oxide aerogels. Excellent results are observed, particularly at high discharge rates. The second study involves the development of electrode fabrication methods, with the objective of increasing electrode loading. Specific capacities in excess of 350 mAh/g are obtained with electrodes containing 10 mg/cm^2.

15. SUBJECT TERMS

Aerogels, vanadium oxide, electrodes

16. SECURITY CLASSIFICATION OF:			17. LIMITATION OF ABSTRACT	18. NUMBER OF PAGES	19a. NAME OF RESPONSIBLE PERSON
a. REPORT	b. ABSTRACT	c. THIS PAGE			
U	U	U	UU	10	19b. TELEPONE NUMBER (Include area code)

Standard Form 298 (Rev. 8-98)
Prescribed by ANSI-Std Z39-18

INTRODUCTION

The present report is related to the development of high surface area aerogels as viable electrode materials for lithium secondary batteries. Aerogels represent a nanoscale, mesoporous material in which both the solid and mesoporous volumes are continuous. The ample porosity provides both molecular accessibility and rapid mass transport via diffusion and for these reasons aerogels have been investigated for heterogeneous catalytic materials for over 50 years. One would expect that this morphology would also be desirable for electrochemical reactions, facilitating electrolyte penetration into the entire aerogel particle through the mesoporous network. However, in research to date, only a few aerogel systems have been investigated as electrochemical materials.[1]

The two topics described in this report are related to the integration of vanadium oxide aerogel materials into reversible electrode structures for secondary lithium batteries. First, we describe our efforts at creating a nanocomposite electrode based on incorporating carbon nanotubes as the electrically conducting network. Because the carbon nanotubes are of the same dimensional scale as the fibrous morphology of V_2O_5 aerogels, the nanocomposite electrode effectively retains the mesoporous morphology of the aerogel and does not impede electrolyte access. In the second part of this report, we detail the procedures for fabricating vanadium oxide aerogel electrodes and characterize the relation between specific capacity and electrode loading.

NANOCOMPOSITE ELECTRODES: VANADIUM OXIDE AEROGEL/CARBON NANOTUBES

<u>Materials and Methods</u>

The vanadium oxide aerogels were prepared using supercritical drying (scd) and ambient drying ('ambigel') methods. For both methods, an alkoxide precursor, vanadyl triisopropoxide, was hydrolyzed in a water-acetone mixture. Details for preparing scd and ambigels of vanadium oxide were reported previously.[2,3] The latter approach involved the use of solvent exchange with a non-polar solvent.

Nanocomposites of vanadium oxide aerogel with single-walled carbon nanotubes (SWNT) were prepared by integrating the nanotubes as part of the sol-gel chemistry. The key feature in preparing the V_2O_5-SWNT nanocomposite cathodes was to use a suspension of SWNT's as the source of diluting solvent (acetone) in preparing the gel. The SWNT's were received in toluene that was gradually replaced with acetone. Although some agglomeration of SWNT's occurred upon adding acetone, the SWNT's remained suspended and did not sediment. This suspension was then combined with the requisite amounts of vanadium alkoxide precursor and water to produce a wet gel. The gelled samples were washed repeatedly in anhydrous acetone and then solvent exchanged with cyclohexane. The cyclohexane was evaporated under ambient conditions to produce the final nanocomposite.

The nanocomposite electrodes were prepared by mixing the V_2O_5-SWNT powder with PVDF in cyclohexane to form a slurry which was then applied to a stainless steel mesh. The electrode material was dried under vacuum at 240°C prior to measurement. For comparison, standard electrodes were prepared using Ketjen Black (KJB) as the conductive additive. The wt% of KJB mixed with the vanadium oxide ambigel was

comparable to that of the SWNT component in the nanocomposite. The same slurry and cathode preparation method was used as described for the nanocomposite. The electrochemical measurements were carried out in an Ar-filled glove box using a conventional three-electrode cell with lithium foil reference and counter electrodes. The electrolyte was 1.0 M lithium perchlorate in anhydrous propylene carbonate.

Results and Discussion

The microstructure of the V_2O_5-SWNT nanocomposite is shown in Figure 1. There is intimate contact between the two phases as several aerogel fibers are intertwined with several SWNT's. The latter are characterized by strongly absorbing regions that are probably the metal nanoparticles used as catalysts during SWNT synthesis. This and other TEM images confirm that the resulting microstructure is the one that was intended. That is, the conductive additive, i.e. carbon nanotubes, establishes extensive contact with the vanadium oxide aerogel at the nanometer dimensional level, and electrolyte access is not likely to be hindered by the presence of the SWNT phase.

BET measurements were used to evaluate pore size, pore volume and surface area for the V_2O_5 aerogel as well as the V_2O_5-SWNT and V_2O_5-KJB composite electrodes. Table 1 shows that the addition of the conductive additive reduces the surface area and pore volume as compared to the pure aerogel. It is important to note that both composites exhibit similar pore volumes, which is an important consideration for electrolyte access. The addition of SWNT has less of an effect on surface area as compared to the KJB.

Cyclic voltammetry was used to analyze the active voltage range for both a SWNT electrode and the V_2O_5-SWNT (17 wt%) nanocomposite electrode (Figure 2). Well defined reduction and oxidation peaks occur at 2.4 and 2.8 Volts, respectively, for the V_2O_5-SWNT electrode while the current response over the entire range is negligible for the SWNT electrode. This result shows that SWNT's are relatively inactive from 4 to 1.5 Volts and do not contribute to the capacity of the V_2O_5-SWNT composite electrodes. This behavior is consistent with reported literature indicating that lithium reacts with SWNT's at voltages less than 1.5 V.[4]

Table 1. Morphology of vanadium oxide aerogel and aerogel composites with conductive additives SWNT and KJB.

Sample	BET surface area (m^2/g)	Avg. Pore Diameter (Angstroms)	Pore volume (cm^3/g)
V_2O_5 aerogel	150	300	0.97
V_2O_5-KJB (17 wt%) Composite	73	310	0.59
V_2O_5-SWNT (5 wt %) Composite	150	205	0.77
V_2O_5-SWNT (17 wt%) Composite	120	190	0.59

One issue we wanted to examine was the influence of electrode morphology on rate capability. In these experiments, the specific discharge capacity (mAh/g) was measured as a function of specific current (mA/g) for two different V_2O_5-SWNT nanocomposite electrodes (9 and 17 wt%) and compared to a traditional electrode (V_2O_5-KJB) which had an equivalent amount of conductive additive (17 wt%). The data (Figure 3) display an interesting trend. At relatively low specific current (112 mA/g) the specific capacities for the different electrodes are approximately the same. The kinetic limitations are insignificant at this discharge rate, and the rather high capacity values for V_2O_5 aerogels ($\sim$ 450 mAh/g) are obtainable. The specific capacities at 112 mA/g are higher, but agree reasonably well with the ones reported in the literature.[5] At slightly higher specific currents (560 mA/g), differences begin to appear. The specific capacity of the V_2O_5-SWNT (17wt%) composite decreases slightly (418 mAh/g) while the V_2O_5-SWNT (9wt%) and the 17wt% KJB cathode are below 400 mAh/g. As the specific current is increased even further, i.e. > 560 mA/g, the specific capacities for both the 9 and 17 wt% V_2O_5-SWNT cathodes are significantly greater than the 17wt% KJB cathode. At 2800 mA/g the specific capacity for the V_2O_5-SWNT (17wt%) nanocomposite cathode is approximately twice as large as the V_2O_5-KJB (17wt%) traditional electrode.

The results shown here are quite interesting in that the basic morphology for each type of electrode was comparable. That is, as shown in Table 1, the pore volume is not substantially different for the various electrodes and, electrolyte access is expected to be similar. It would seem then that the low electrical resistance arising from the intimate contact between the nanotubes and the vanadium oxide fibers must be an important consideration for achieving high rate capability. At this time we have made only qualitative measurements of the electrical resistance of the electrodes. It is apparent that electrodes prepared with carbon nanotubes as the conductive network exhibit substantially lower resistivities (by about a factor of 4) compared to electrodes containing the same weight fraction of the KJB additive. It is not surprising, therefore, that the performance of the cathodes with a lesser amount of SWNT (i.e., 9 wt %) is comparable or better than the traditional electrodes containing nearly twice as much KJB (17 wt %).

Galvanostatic cycling experiments for the V_2O_5-SWNT electrodes are underway and initial results for the 17wt% composite cathodes are shown in Figure 6. These cathodes were cycled between 4.0 and 1.5V at a discharge rate of 560 mA/g and charge rate of 280 mA/g. The first and twentieth discharge curves are shown in Figure 6. These electrodes did not exhibit any capacity loss over the twenty cycles tested and delivered over 400 mAh/g per cycle. It is interesting to note that cycling data for similar vanadium oxide aerogel cathodes that used KJB as the conductive additive exhibited a significant capacity decline over twenty cycles with even slower discharge rates.[5] In view of the excellent mechanical properties of carbon nanotubes, it is tempting to speculate that the SWNT's may actually reinforce the electrode structure, enhance its integrity and ensure that electrical contact is maintained throughout cycling. Future work is necessary to determine whether such mechanical effects do indeed influence cycling behavior.

3

FABRICATION AND CHARACTERIZATION OF
VANADIUM OXIDE AEROGEL ELECTRODES

In this part of the program, experiments were carried out using electrodes fabricated from a slurry, consisting of V_2O_5 aerogel powder, carbon black and a polymer binder, that was air-brushed onto on a stainless steel mesh. The principal objective was to determine how the specific capacity for lithium was influenced by the weight of the electrode (i.e., its loading).

Materials and Methods

The various fabrication and testing parameters are as follows:
- Vanadium oxide aerogel was synthesized by the ambigel method using cyclohexane
- Ketjen Black was used as the carbon black
- Binder was primarily PVDF (polyvinylidene difluoride); a few experiments used PAN (polyacrylonitrile)
- The stainless steel mesh was from Alfa Aesar (#13477); wire diameter = 0.028 mm.; width opening = 0.036 mm.
- Solvent was cyclohexane (C_6H_{12}); a few experiments used propylene carbonate (PC)
- An airbrush was used to spray the slurry onto a 1 cm x 1 cm area of the mesh
- After deposition, electrodes were dried initially with a heat gun ($T > 200°C$) to drive off most of the solvent
- Samples were then dried at about 200°C for 15 min. in air, then 15 min. in vacuum to evaporate any remaining solvent
- Electrochemical testing: 3-electrode cell with V_2O_5/KJB working electrode and lithium foil reference and counter electrodes. Electrolyte: 1 M $LiClO_4$ in PC. Electrodes operated between 4.0 and 1.5 V. Discharge rate of C/5; charge rate of C/10

Results and Discussion

The salient experimental results are shown in Table 2 which show the loadings (in mg/cm^2) for different preparations and the resulting discharge capacities. In general, the specific capacity remained in the 300 to 400 mAh/g range for loadings up to 10 mg/cm^2. Variations in electrode fabrication are noted in the comments. One of the variations to the standard method included changing the solvent from cyclohexane to polypropylene carbonate (samples G21, G22 and G23). Both the V_2O_5 and the KJB mix better in PC than in cyclohexane. Using PC instead of cyclohexane also made it easier to control how quickly the solvent dries as cyclohexane evaporates very rapidly from the sample. G23 had the additional variable of having been fabricated by smearing slurry on both sides of the mesh (instead of using the air brush) in an attempt to increase the amount of loading. This type of fabrication did not effectively increase the amount of loading.

For sample G25, the binder was changed from PVDF to PAN. PAN has a higher melting temperature ($T_m \sim 240°C$) than PVDF ($T_m \sim 170°C$). This ensures that the binder will survive the drying step. As Table 2 shows, this change did not affect the capacity of the electrode.

4

Sample	Loading [mg/cm^2]	Specific capacity (mAh/g)			Comments
		1st disch.	2nd disch.	3rd disch.	
Table 2: Specific capacity on discharge for different electrode loading levels					
80% VAG, 15% CB, 5% PVDF					
G13	9.0	292	276	272	4 V to 1.8 V
	7.9		327	327	
G20	8.1	435	435	447	
G21	7.7	287	286	282	1:4 C_6H_{12} to PC sol'n
G22	4.4	410	403	394	all PC sol'n
G23	4.9	370	365	359	PC sol'n and slurry
80% VAG, 15% CB, 5% PAN					
G25	10.1	376	366	362	

Figure 5 shows the first three cycles for a typical discharge curve. A plot summarizing the effect of electrode loading on capacity is shown in Figure 6. Certainly there is a bit of scatter in the data which we attribute to variations in electrode quality (cracking, variable thickness), inconsistent drying methods and inadvertent exposure to water. Nonetheless, it is evident that there is no difficulty in achieving specific capacities in the range of 300 to 400 mAh/g. One significant result shown here is that the highest loaded sample (G25) also exhibits a very respectable specific capacity (376 mAh/g). This suggests that future studies should explore the use of PAN as a binder.

We carried out only a few microstructure studies of the electrodes and thus, the electrodes shown in Figure 7 should be considered as initial results and not as a trend. SEM images of the electrodes prepared using PVDF (left) and PAN (right) are shown. The loading for the PVDF electrode is 13 mg/cm^2 while that for the PAN electrode is 10 mg/cm^2. Since we did not do an extensive study of electrode morphology, we cannot be sure that PAN electrodes necessarily lead to more cracks. However, we believe that the presence of cracks is one of the factors contributing to the variable behavior shown for the specific capacity.

CONCLUSIONS

The use of vanadium oxide aerogels in electrode structures for lithium secondary batteries is just at its inception. We consider it of utmost importance that these materials retain their mesoporous morphology when incorporated in the actual electrode as this feature provides electrolyte access to the solid phase, leading to the excellent specific capacities exhibited by these materials.

This study has considered two different aspects of integrating aerogels into electrode structures. First, we described methods for providing an electronically conducting network. We found that nanocomposite electrodes based on the incorporation of carbon nanotubes led to excellent results. The vanadium oxide aerogel/carbon nanotube electrodes retained high specific capacity at high discharge rates, a feature

which may be due to the inherent nature of aerogels – a combination of battery-like and capacitor-like behaviors. The experiments showing that these electrodes exhibited no decrease in capacity with cycling suggest that the mechanical properties of nanotubes may be instrumental in avoiding the capacity fade behavior commonly observed with the vanadium oxide system. The second part of this work considered methods for fabricating electrodes with an emphasis on determining whether specific capacity could be retained as electrodes became "heavier". Although there is scatter in the data, there is no question that high capacity can be retained with electrodes containing as much as 10 mg/cm^2. The study also indicated that the role of the binder should be more thoroughly investigated as the use of PAN gave excellent results.

REFERENCES

1. D.R. Rolison and B. Dunn, *J. Mater. Chem.* accepted for publication.
2. F. Chaput, B. Dunn, P. Fuqua and K. Salloux, *J. Non-Cryst. Solids* **188**, 11 (1995).
3. J.H. Harreld, W. Dong and B. Dunn, *Mater. Res. Bull.* **33**, 561 (1998).
4. A.S. Claye, J.E. Fisher, C.B. Huffman, A.G. Rinzler and R. Smalley, *J. Electrochem. Soc*, **147**, 2845 (2000)
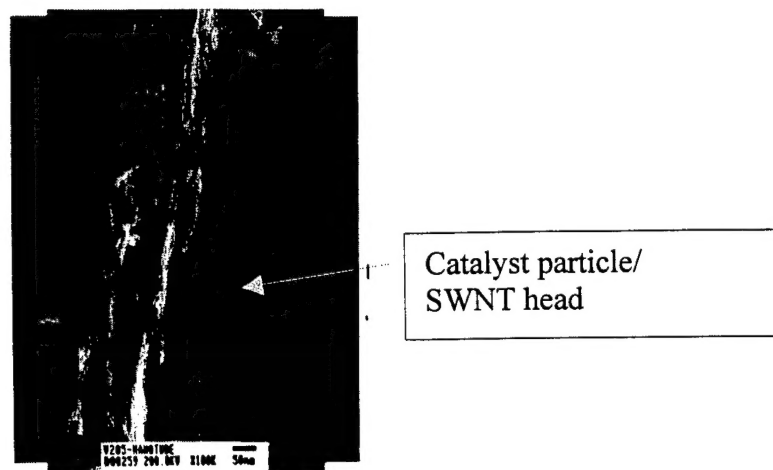5. F. Coustier, S. Passerini and W.H. Smyrl, *J. Electrochem. Soc.*, **145**, L73 (1998)

Figure 1. TEM image of the microstructure for the V_2O_5 aerogel - SWNT composite.
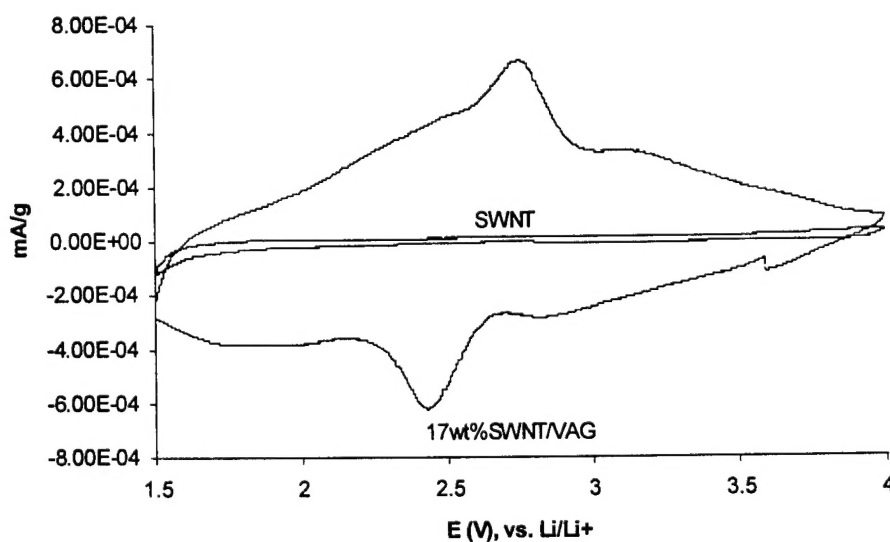The dimension bar is 50 nm.

Figure 2. Voltammograms for SWNT and the V_2O_5-SWNT (17 wt%) nanocomposite.
The intercalation/deintercalation peaks for the nanocomposite are quite prominent. The
voltammogram for the SWNT indicates that the carbon nanotubes do not contribute to the
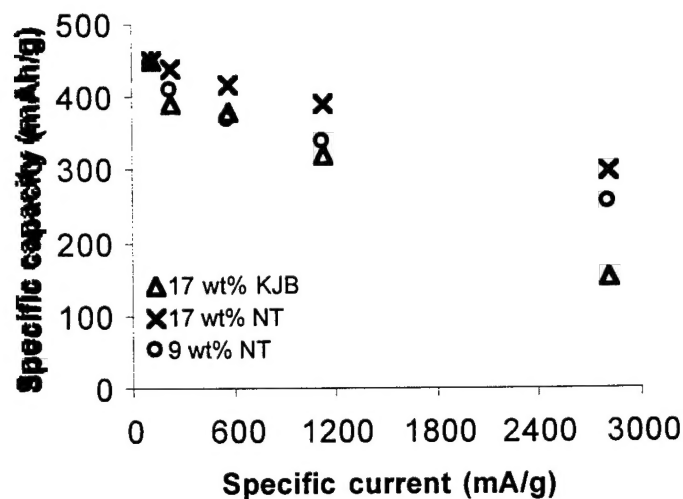capacity of the composite electrode.

Figure 3. Specific capacity as a function of rate for V_2O_5-SWNT nanocomposite electrodes with 9 and 17 wt% SWNT compared to a traditional electrode (V_2O_5-KJB) which had an equivalent amount of conductive additive (17 wt%).
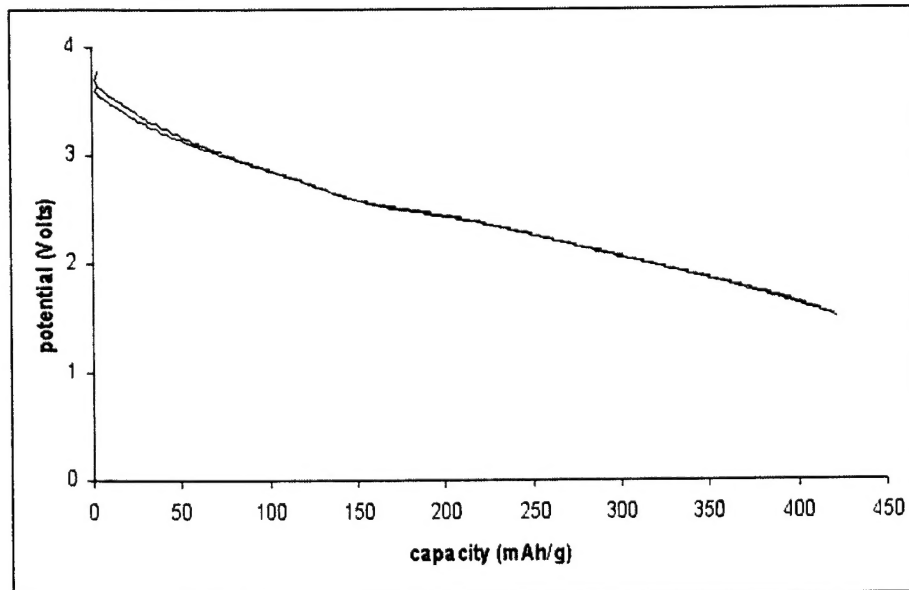

Figure 4. Discharge curves for V_2O_5-SWNT nanocomposite electrode containing 17 wt% SWNT's. The first and twentieth discharge profiles are shown. No capacity loss is evident. The cells were cycled at 560 mA/g.
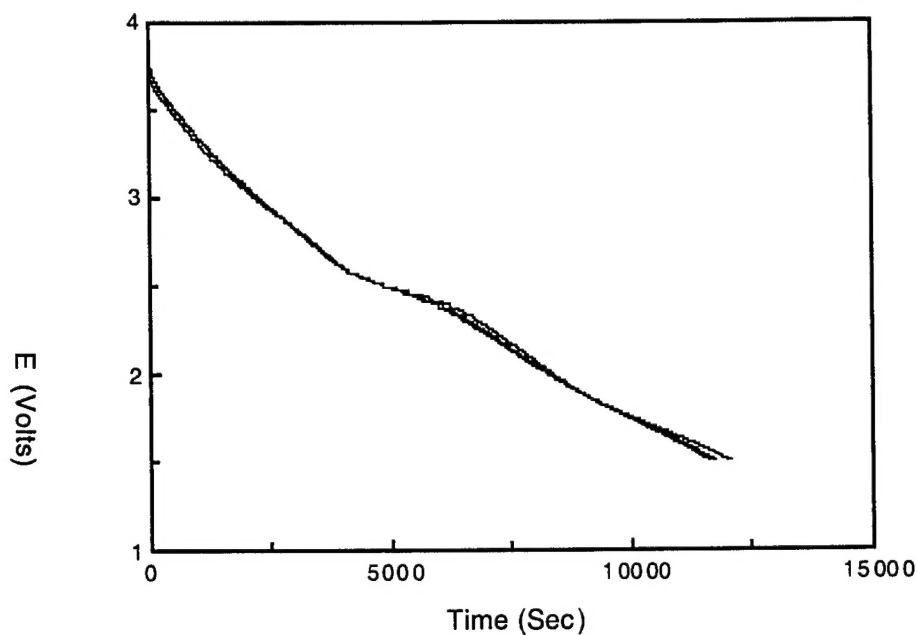
8

Figure 5. Discharge curve for the first three cycles of an aerogel electrode. The decrease in capacity for these cycles is less than 5%.
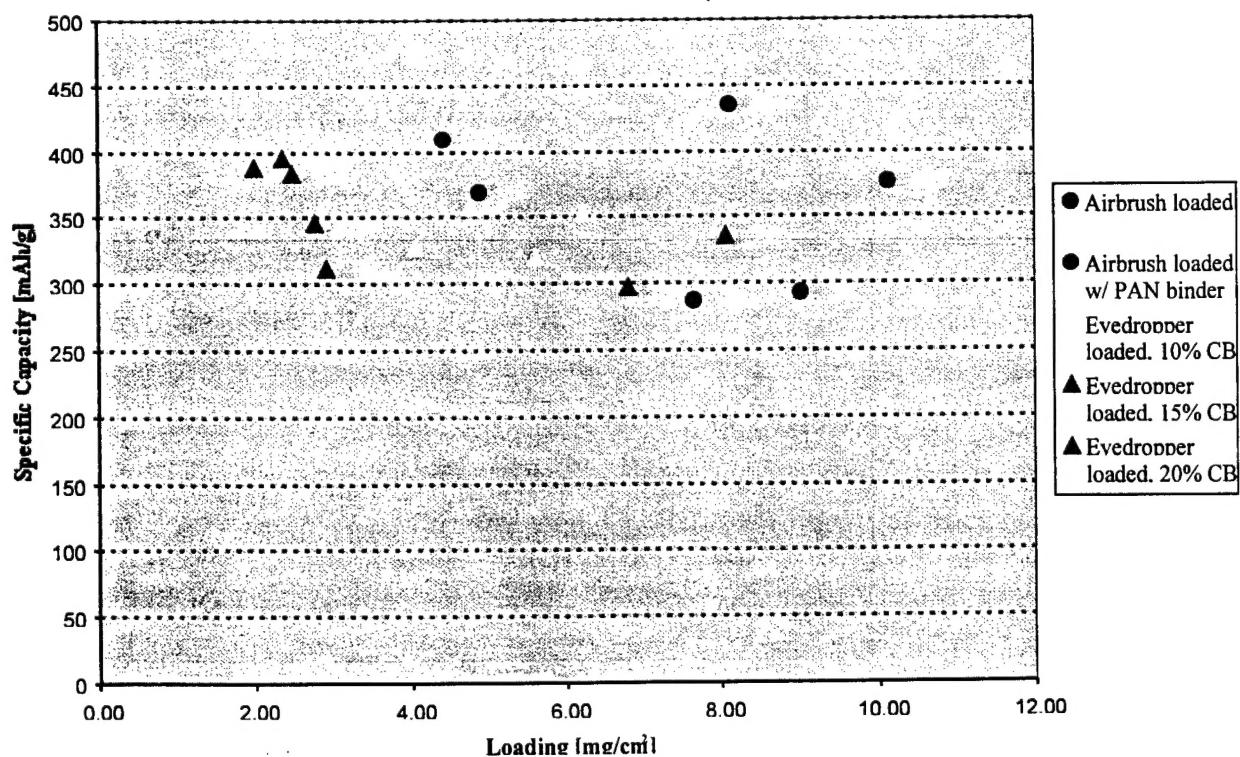

Figure 6. Specific discharge capacity (1st cycle) for aerogel electrodes prepared by various methods. The "Eyedropper loaded" samples represents earlier work when we were developing the airbrush deposition method.
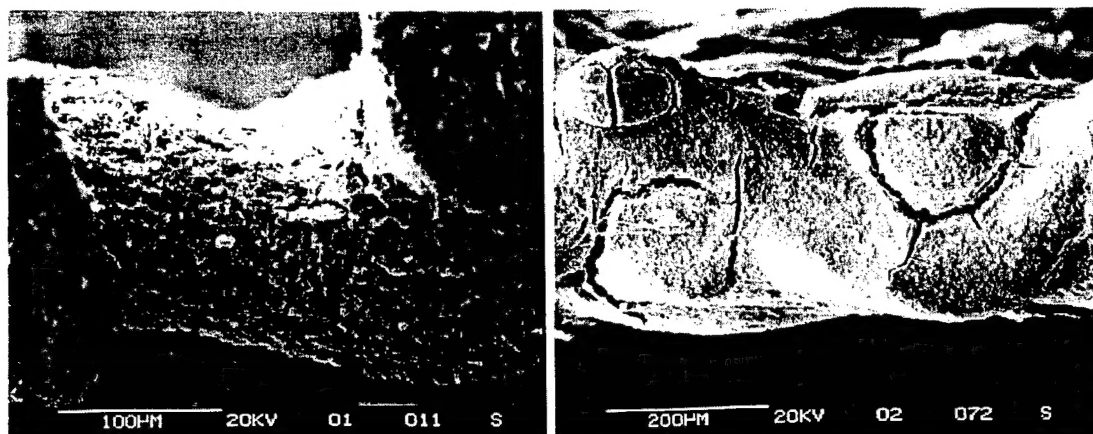
Figure 7. SEM of electrodes fabricated with PVDF binder (left) and PAN binder (right). There are more cracks evident in the electrode prepared with PAN.